[November, 1991] Bull. Chem. Soc. Jpn., 64, 3215—3223 (1991)

Soccerane Derivatives of Given Symmetries

Shinsaku Fujita
Research Laboratories, Ashigara, Fuji Photo Film Co., Ltd.,
Minami-Ashigara, Kanagawa 250-01
(Received November 26, 1990)

Symmetrical properties of soccerane and its derivatives are discussed in the light of subduction of coset representations (CRs). The 60 vertices of soccerane are equivalent and construct a single orbit governed by the CR, $\mathbf{I}_h(/\mathbf{C}_s)$. This orbit is divided into several orbits in the respective derivative, where the mode of the division is controlled by the subduction. The number of derivatives with a given formula and a given subsymmetry is calculated in terms of unit subduced cycle indices, which are derived from the subduction.

Hydrocarbons of high symmetries and related compounds have attracted continuous attention of organic chemists because of their potential properties.[1] Among them, a fully unsaturated C_{60} compound of $\mathbf{I}_h$ symmetry has once been mentioned by Ōsawa[2] as a theoretically interesting compound. The corresponding saturated $C_{60}H_{60}$-hydrocarbon (**1**) has been called "footballane" or "soccerane" by Castells and Serratosa.[3] They pointed out: "Since the synthesis of dodecahedrane has been recently accomplished by Paquette and his coworkers at Ohio State University, the synthesis of soccerane appears as the next goal". They later gave this complex hydrocarbon the IUPAC name,[4] i. e., hentriacontacyclo[$29.29.0.0^{2,14}.0^{3,29}.0^{4,27}.0^{5,13}.0^{6,25}.0^{7,12}.0^{8,23}.0^{9,21}.0^{10,18}.0^{11,16}.0^{15,60}.0^{17,58}.0^{19,56}.0^{20,54}.0^{22,52}.0^{24,50}.0^{26,49}.0^{28,47}.0^{30,45}.0^{32,44}.0^{33,59}.0^{34,57}.0^{35,43}.0^{36,55}.0^{37,42}.0^{38,53}.0^{39,51}.0^{40,48}.0^{41,46}$]hexacontane.

Recently, a C_{60} peak has been observed in a laser vaporization of graphite by Kroto et al.,[5a] where the peak was assigned to formation of the above $\mathbf{I}_h$ molecule (a C_{60} carbon cluster).[6] This paper has stimulated a large number of theoretical studies on this carbon cluster.[7] Other compounds of $\mathbf{I}_h$ symmetry (Fig. 1) have also attracted theoretical attention of chemists.[8] A brief review has summarized predicted properties of these related compounds.[9] Geometrical properties of soccerane and other $\mathbf{I}_h$-molecules have been discussed.[10] Since soccerane has been so far detected only by physicochemical analysis, total syntheses of such high-symmetry molecules are challenging targets from the viewpoint of synthetic organic chemistry.

Since the $\mathbf{I}_h$ symmetry contains various unusual subsymmetries, derivatization of soccerane ($C_{60}H_{60}$) by substituting an appropriate set of atoms for the same number of hydrogen atoms produces molecules of the subsymmetries, which will be further targets of synthetic organic chemistry. In this connection, the number of derivatives of a given subsymmetry of this series will be of interest to organic chemists. Hosoya[10] has enumerated such soccerane derivatives by using Pólya's theorem.[11] This enumeration is, however, concerned with their molecular formulas and not with their symmetries.

We have reported a systematic enumeration of molecules in terms of unit subduced cycle indices (USCIs).[12,13] This method requires a table of marks (or the inverse) due to Burnside[14] and a table of USCIs introduced by us.[12] We have presented such tables for $\mathbf{C}_2$, $\mathbf{C}_{2v}$, $\mathbf{C}_{3v}$, $\mathbf{D}_2$, $\mathbf{D}_{2d}$, $\mathbf{D}_{2h}$, $\mathbf{D}_3$, $\mathbf{D}_{3h}$, $\mathbf{T}$, and $\mathbf{T}_d$ as well as their applications to various enumerations.[15] We have recently reported construction of such tables for the $\mathbf{I}_h$ group and applications to enumeration of dodecahedrane derivatives.[16] However, the advantage of the USCI approach for enumeration has not been fully investigated, inasmuch as the enumerations have been limited within rather simple molecules. The present paper deals with the enumeration of isomers derived from soccerane in order to exemplify the advantage and generality of the USCI approach.

1. Orbits in $\mathbf{I}_h$ Molecules. Figure 1 collects the soccerane skeleton and the related ones of $\mathbf{I}_h$ symmetry. We first examine the symmetrical properties of the skeletons. Any skeleton has several sets of equivalent positions (vertices, edges or faces). These sets are called *orbits* in accord with the terminology of permutation group. The symmetry properties of each orbit is characterized by the corresponding coset representaion (CR).[17,18] The CR is represented by the symbol $\mathbf{G}(/\mathbf{G}_i)$ that is based on a coset decomposition of $\mathbf{G}$ by $\mathbf{G}_i$, where $\mathbf{G}$ is the point group of the skeleton and $\mathbf{G}_i$ is its subgroup.

Since the $\mathbf{I}_h$ group of order 120 posesses a set of subgroups, SSG=\{$\mathbf{C}_1$, $\mathbf{C}_2$, $\mathbf{C}_s$, $\mathbf{C}_i$, $\mathbf{C}_3$, $\mathbf{D}_2$, $\mathbf{C}_{2v}$, $\mathbf{C}_{2h}$, $\mathbf{C}_5$, $\mathbf{D}_3$,

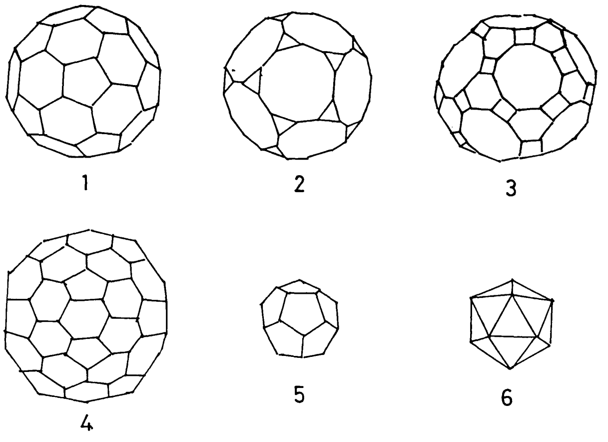

Fig. 1. Skeletons of $\mathbf{I}_h$ symmetry.

Table 1. Orbits of Several Compounds of $\mathbf{I}_h$ Symmetry

Compound	Objects	No. of objects	Coset representation	SCR notation
1	Vertices [5.6.6]	60	$\mathbf{I}_h(/\mathbf{C}_s)$	$\mathbf{I}_h[/\mathbf{C}_s([5.6.6]_{60})]$
	Edges [6:6]	60	$\mathbf{I}_h(/\mathbf{C}_s)$	
	Edges [5:6]	30	$\mathbf{I}_h(/\mathbf{C}_{2v})$	
	Hexagonal faces	20	$\mathbf{I}_h(/\mathbf{C}_{3v})$	
	Pentagonal faces	12	$\mathbf{I}_h(/\mathbf{C}_{5v})$	
2	Vertices [3.10.10]	60	$\mathbf{I}_h(/\mathbf{C}_s)$	$\mathbf{I}_h[/\mathbf{C}_s([3.10.10]_{60})]$
	Edges [3:10]	60	$\mathbf{I}_h(/\mathbf{C}_s)$	
	Edges [10:10]	30	$\mathbf{I}_h(/\mathbf{C}_{2v})$	
	Trigonal faces	20	$\mathbf{I}_h(/\mathbf{C}_{3v})$	
	Decagonal faces	12	$\mathbf{I}_h(/\mathbf{C}_{5v})$	
3	Vertices [4.6.10]	120	$\mathbf{I}_h(/\mathbf{C}_1)$	$\mathbf{I}_h[/\mathbf{C}_{3v}([4.6.10]_{120})]$
	Edges [4:6]	60	$\mathbf{I}_h(/\mathbf{C}_s)$	
	Edges [4:10]	60	$\mathbf{I}_h(/\mathbf{C}_s)$	
	Edges [10:10]	60	$\mathbf{I}_h(/\mathbf{C}_s)$	
	Tetragonal faces	30	$\mathbf{I}_h(/\mathbf{C}_{2v})$	
	Hexagonal faces	20	$\mathbf{I}_h(/\mathbf{C}_{3v})$	
	Decagonal faces	12	$\mathbf{I}_h(/\mathbf{C}_{5v})$	
4	Vertices [5.6.6]	60	$\mathbf{I}_h(/\mathbf{C}_s)$	$\mathbf{I}_h[/\mathbf{C}_s([5.6.6]_{60})$;
	Vertices [6.6.6]	20	$\mathbf{I}_h(/\mathbf{C}_{3v})$	$/\mathbf{C}_{3v}([6.6.6]_{20})]$
	Edges [6:6]	60	$\mathbf{I}_h(/\mathbf{C}_s)$	
	Edges [5:6]	60	$\mathbf{I}_h(/\mathbf{C}_s)$	
	Hexagonal faces	30	$\mathbf{I}_h(/\mathbf{C}_{2v})$	
	Pentagonal faces	12	$\mathbf{I}_h(/\mathbf{C}_{5v})$	
5	Vertices [5.5.5]	20	$\mathbf{I}_h(/\mathbf{C}_{3v})$	$\mathbf{I}_h[/\mathbf{C}_{3v}([5.5.5]_{20})]$
	Edges [5:5]	30	$\mathbf{I}_h(/\mathbf{C}_{2v})$	
	Pentagonal faces	12	$\mathbf{I}_h(/\mathbf{C}_{5v})$	
6	Vertices [3.3.3.3.3.]	12	$\mathbf{I}_h(/\mathbf{C}_{5v})$	$\mathbf{I}_h[/\mathbf{C}_{5v}([3.3.3.3.3]_{12})]$
	Edges [3:3]	30	$\mathbf{I}_h(/\mathbf{C}_{2v})$	
	Triginal faces	20	$\mathbf{I}_h(/\mathbf{C}_{3v})$	

$\mathbf{C}_{3v}$, $\mathbf{C}_{3i}$, $\mathbf{D}_{2h}$, $\mathbf{D}_5$, $\mathbf{C}_{5v}$, $\mathbf{C}_{5i}$, $\mathbf{T}$, $\mathbf{D}_{3d}$, $\mathbf{D}_{5d}$, $\mathbf{T}_h$, $\mathbf{I}$, $\mathbf{I}_h\}$, the corresponding set of CRs is designated to be SCR=$\{\mathbf{I}_h(/\mathbf{C}_1)$, $\mathbf{I}_h(/\mathbf{C}_2)$, $\mathbf{I}_h(/\mathbf{C}_s)$, $\mathbf{I}_h(/\mathbf{C}_i)$, $\mathbf{I}_h(/\mathbf{C}_3)$, $\mathbf{I}_h(/\mathbf{D}_2)$, $\mathbf{I}_h(/\mathbf{C}_{2v})$, $\mathbf{I}_h(/\mathbf{C}_{2h})$, $\mathbf{I}_h(/\mathbf{C}_5)$, $\mathbf{I}_h(/\mathbf{D}_3)$, $\mathbf{I}_h(/\mathbf{C}_{3v})$, $\mathbf{I}_h(/\mathbf{C}_{3i})$, $\mathbf{I}_h(/\mathbf{D}_{2h})$, $\mathbf{I}_h(/\mathbf{D}_5)$, $\mathbf{I}_h(/\mathbf{C}_{5v})$, $\mathbf{I}_h(/\mathbf{C}_{5i})$, $\mathbf{I}_h(/\mathbf{T})$, $\mathbf{I}_h(/\mathbf{D}_{3d})$, $\mathbf{I}_h(/\mathbf{D}_{5d})$, $\mathbf{I}_h(/\mathbf{T}_h)$, $\mathbf{I}_h(/\mathbf{I})$, $\mathbf{I}_h(/\mathbf{I}_h)\}$.

Table 1 lists orbits of each skeleton shown in Fig. 1. We have reported a method of assigning a CR to each orbit[17,18] as well as data necessary to this task.[16] For simplicity's sake, we consider the soccerane skeleton to be a truncated icosahedron, which has 60 vertices, 90 edges, and 32 faces. In order to illustrate a procedure of the assignment, we examine the 60 vertices of **1**, which are equivalent and construct a single orbit. We first count fixed points (vertices) for each subgroup during all of the operations contained in the subgroup, affording a fixed-point vector (FPV). We thus obtain an FPV= (60 0 4 0 0 0 0 0 0 0 0 0 0 0 0 0 0 0 0 0 0 0) for the vertices. This vector is multiplied by the inverse of a mark table for $\mathbf{I}_h$ group (Table 2). The resulting vector (0 0 1 0 0 0 0 0 0 0 0 0 0 0 0 0 0 0 0 0 0 0) shows the multiplicities of the subgroups listed in the SSG; in this case, there appears only one $\mathbf{I}_h(/\mathbf{C}_s)$ orbit. If the symbol $\mathbf{P}_{1(\mathrm{vertex})}$ denotes a permutation representation concerning the 60 vertices, we have

$$\mathbf{P}_{1(\mathrm{vertex})} = \mathbf{I}_h(/\mathbf{C}_s). \tag{1}$$

Note that the size of the orbit is equal to $|\mathbf{I}_h|/|\mathbf{C}_s|=120/2=60$. Since a 5-membered ring and two 6-membered rings meet at each vertex, we refer to this vertex as a [5.6.6] vertex. Thereby, we can obtain the SCR notation,[17] $\mathbf{I}_h[/\mathbf{C}_s([5.6.6]_{60})]$ for this skeleton, where the CR and its members are indicated.

There are two kinds of edges in **1**, which construct distinct orbits. With respect to these edges, we have an FPV=(90 2 8 0 0 0 2 0 0 0 0 0 0 0 0 0 0 0 0 0 0 0). This vector is multiplied by the inverse (Table 2), producing a row vector, (0 0 1 0 0 0 1 0 0 0 0 0 0 0 0 0 0 0 0 0 0 0). This corresponds to the following equation,

$$\mathbf{P}_{1(\mathrm{edge})} = \mathbf{I}_h(/\mathbf{C}_s) + \mathbf{I}_h(/\mathbf{C}_{2v}), \tag{2}$$

in which the symbol $\mathbf{P}_{1(\mathrm{edge})}$ denotes a permutation representation of the 90 edges. Note that the degree of $\mathbf{I}_h(/\mathbf{C}_s)$ is equal to $|\mathbf{I}_h|/|\mathbf{C}_s|=120/2=60$ and that of $\mathbf{I}_h(/\mathbf{C}_{2v})$ is equal to $|\mathbf{I}_h|/|\mathbf{C}_{2v}|=120/4=30$. If the symbol [6:6] denotes an edge at which two 6-membered rings fuse, Eq. 2 concludes that the sixty [6:6]edges in **1** construct an orbit that is subject to $\mathbf{I}_h(/\mathbf{C}_s)$. Similarly,

Table 2. The Inverse of the Mark Table of $\mathbf{I}_h$ Group

	Coset representation[a)]																						
	$\mathbf{C}_1$	$\mathbf{C}_2$	$\mathbf{C}_s$	$\mathbf{C}_i$	$\mathbf{C}_3$	$\mathbf{D}_2$	$\mathbf{C}_{2v}$	$\mathbf{C}_{2h}$	$\mathbf{C}_5$	$\mathbf{D}_3$	$\mathbf{C}_{3v}$	$\mathbf{C}_{3i}$	$\mathbf{D}_{2h}$	$\mathbf{D}_5$	$\mathbf{C}_{5v}$	$\mathbf{C}_{5i}$	$\mathbf{T}$	$\mathbf{D}_{3d}$	$\mathbf{D}_{5d}$	$\mathbf{T}_h$	$\mathbf{I}$	$\mathbf{I}_h$	Sum[b)]
$\mathbf{C}_1$	$\frac{1}{120}$	0	0	0	0	0	0	0	0	0	0	0	0	0	0	0	0	0	0	0	0	0	$\frac{1}{120}$
$\mathbf{C}_2$	$-\frac{1}{8}$	$\frac{1}{4}$	0	0	0	0	0	0	0	0	0	0	0	0	0	0	0	0	0	0	0	0	$\frac{1}{8}$
$\mathbf{C}_s$	$-\frac{1}{8}$	0	$\frac{1}{4}$	0	0	0	0	0	0	0	0	0	0	0	0	0	0	0	0	0	0	0	$\frac{1}{8}$
$\mathbf{C}_i$	$-\frac{1}{120}$	0	0	$\frac{1}{60}$	0	0	0	0	0	0	0	0	0	0	0	0	0	0	0	0	0	0	$\frac{1}{120}$
$\mathbf{C}_3$	$-\frac{1}{12}$	0	0	0	$\frac{1}{4}$	0	0	0	0	0	0	0	0	0	0	0	0	0	0	0	0	0	$\frac{1}{6}$
$\mathbf{D}_2$	$\frac{1}{12}$	$-\frac{1}{4}$	0	0	0	$\frac{1}{6}$	0	0	0	0	0	0	0	0	0	0	0	0	0	0	0	0	0
$\mathbf{C}_{2v}$	$\frac{1}{4}$	$-\frac{1}{4}$	$-\frac{1}{2}$	0	0	0	$\frac{1}{2}$	0	0	0	0	0	0	0	0	0	0	0	0	0	0	0	0
$\mathbf{C}_{2h}$	$\frac{1}{4}$	$-\frac{1}{4}$	$-\frac{1}{4}$	$-\frac{1}{4}$	0	0	0	$\frac{1}{2}$	0	0	0	0	0	0	0	0	0	0	0	0	0	0	0
$\mathbf{C}_5$	$-\frac{1}{20}$	0	0	0	0	0	0	0	$\frac{1}{4}$	0	0	0	0	0	0	0	0	0	0	0	0	0	$\frac{1}{5}$
$\mathbf{D}_3$	$\frac{1}{4}$	$-\frac{1}{2}$	0	0	$-\frac{1}{4}$	0	0	0	0	$\frac{1}{2}$	0	0	0	0	0	0	0	0	0	0	0	0	0
$\mathbf{C}_{3v}$	$\frac{1}{4}$	0	$-\frac{1}{2}$	0	$-\frac{1}{4}$	0	0	0	0	0	$\frac{1}{2}$	0	0	0	0	0	0	0	0	0	0	0	0
$\mathbf{C}_{3i}$	$\frac{1}{12}$	0	0	$-\frac{1}{6}$	$-\frac{1}{4}$	0	0	0	0	0	0	$\frac{1}{2}$	0	0	0	0	0	0	0	0	0	0	$\frac{1}{6}$
$\mathbf{D}_{2h}$	$-\frac{1}{3}$	$\frac{1}{2}$	$\frac{1}{2}$	$\frac{1}{6}$	0	$-\frac{1}{6}$	$-\frac{1}{2}$	$-\frac{1}{2}$	0	0	0	0	$\frac{1}{3}$	0	0	0	0	0	0	0	0	0	0
$\mathbf{D}_5$	$\frac{1}{4}$	$-\frac{1}{2}$	0	0	0	0	0	0	$-\frac{1}{4}$	0	0	0	0	$\frac{1}{2}$	0	0	0	0	0	0	0	0	0
$\mathbf{C}_{5v}$	$\frac{1}{4}$	0	$-\frac{1}{2}$	0	0	0	0	0	$-\frac{1}{4}$	0	0	0	0	0	$\frac{1}{2}$	0	0	0	0	0	0	0	0
$\mathbf{C}_{5i}$	$\frac{1}{20}$	0	0	$-\frac{1}{10}$	0	0	0	0	$-\frac{1}{4}$	0	0	0	0	0	0	$\frac{1}{2}$	0	0	0	0	0	0	$\frac{1}{5}$
$\mathbf{T}$	$\frac{1}{6}$	0	0	0	$-\frac{1}{2}$	$-\frac{1}{6}$	0	0	0	0	0	0	0	0	0	0	$\frac{1}{2}$	0	0	0	0	0	0
$\mathbf{D}_{3d}$	$-\frac{1}{2}$	$\frac{1}{2}$	$\frac{1}{2}$	$\frac{1}{2}$	$\frac{1}{2}$	0	0	-1	0	$-\frac{1}{2}$	$-\frac{1}{2}$	$-\frac{1}{2}$	0	0	0	0	0	1	0	0	0	0	0
$\mathbf{D}_{5d}$	$-\frac{1}{2}$	$\frac{1}{2}$	$\frac{1}{2}$	$\frac{1}{2}$	0	0	0	-1	$\frac{1}{2}$	0	0	0	0	$-\frac{1}{2}$	$-\frac{1}{2}$	$-\frac{1}{2}$	0	0	1	0	0	0	0
$\mathbf{T}_h$	$-\frac{1}{6}$	0	0	$\frac{1}{3}$	$\frac{1}{2}$	$\frac{1}{6}$	0	0	0	0	0	-1	$-\frac{1}{3}$	0	0	0	$-\frac{1}{2}$	0	0	1	0	0	0
$\mathbf{I}$	$-\frac{1}{2}$	1	0	0	$\frac{1}{2}$	0	0	0	0	$-\frac{1}{2}$	0	0	0	$-\frac{1}{2}$	0	0	$-\frac{1}{2}$	0	0	0	$\frac{1}{2}$	0	0
$\mathbf{I}_h$	$\frac{1}{2}$	-1	0	-1	$-\frac{1}{2}$	0	0	2	0	$\frac{1}{2}$	0	1	0	$\frac{1}{2}$	0	0	$\frac{1}{2}$	-1	-1	-1	$-\frac{1}{2}$	1	0

a) The symbol $\mathbf{G}_i$ is an abbreviation of $\mathbf{I}_h(/\mathbf{G}_i)$, where $\mathbf{G}_1=\mathbf{C}_1$, $\mathbf{G}_2=\mathbf{C}_2$, $\cdots$, $\mathbf{G}_s=\mathbf{I}_h$. For example, we here use $\mathbf{C}_2$ for $\mathbf{I}_h(/\mathbf{C}_2)$. b) Sum$=\sum_{j=1}^{s}\overline{m}_{ji}$.

thirty [5:6]edges are subject to $\mathbf{I}_h(/\mathbf{C}_{2v})$.

The 32 faces of the molecule (**1**) give an FPV=(32 0 8 0 2 0 0 0 2 0 2 0 0 0 2 0 0 0 0 0 0 0). The multiplication of the FPV by the inverse (Table 2) affords a row vector (0 0 0 0 0 0 0 0 0 0 1 0 0 0 1 0 0 0 0 0 0 0), which indicates the appearence of $\mathbf{I}_h(/\mathbf{C}_{3v})$ and $\mathbf{I}_h(/\mathbf{C}_{5v})$. Hence, the 32 faces are characterized by

$$\mathbf{P}_{1(\text{face})}=\mathbf{I}_h(/\mathbf{C}_{3v})+\mathbf{I}_h(/\mathbf{C}_{5v}). \tag{3}$$

Since $|\mathbf{I}_h|/|\mathbf{C}_{3v}|=120/6=20$ and $|\mathbf{I}_h|/|\mathbf{C}_{5v}|=120/10=12$, Eq. 3 means that 20 hexagonal faces belong to an orbit governed by $\mathbf{I}_h(/\mathbf{C}_{3v})$; and that the remaining 12 pentagonal faces construct an orbit governed by $\mathbf{I}_h(/\mathbf{C}_{5v})$.

In a similar way, the orbits of the other skeletons are assigned to the respective CRs (Table 1). It should be noted that another C_{60} icosahedral skeleton (**2**) has equal numbers of vertices, edges, and faces as compared with **1** and that these are subject to the same CRs. The latter skeleton (**2**) can be differentiated from **1** by the SCR notation, $\mathbf{I}_h[/\mathbf{C}_s([3.10.10]_{60})]$.

2. Subduction of the $\mathbf{I}_h(/\mathbf{C}_s)$ Orbit. The replacement of hydrogen atoms of **1** by other atoms produces a derivative of **1** that belongs to a subsymmetry of $\mathbf{I}_h$. Such a desymmetrization process is characterized in terms of subduction of the corresponding CR.[18)] For manipulating the soccerane skeleton (**1**), the $\mathbf{I}_h(/\mathbf{C}_s)$ CR is subduced into every subgroup. In order to illustrate such a subduction, let us examine $\mathbf{I}_h(/\mathbf{C}_s)\downarrow\mathbf{C}_{2v}$, which denotes the subduction of the $\mathbf{I}_h(/\mathbf{C}_s)$ representation into the $\mathbf{C}_{2v}$ group. The $\mathbf{I}_h(/\mathbf{C}_s)$ row of a mark table is equal to the row vector, FPV=(60 0 4 0 0 0 0 0 0 0 0 0 0 0 0 0 0 0 0 0 0 0), the elements of which are aligned in the order of the SSG.[19)] Since the SSG of the $\mathbf{C}_{2v}$ group is represented by SSG'={$\mathbf{C}_1$, $\mathbf{C}_2$, $\mathbf{C}_s$, $\mathbf{C}'_s$, $\mathbf{C}_{2v}$}, we can obtain a row vector (60 0 4 4 0) by selecting from the FPV the values corresponding to the SSG'. Note that the value 4 for the $\mathbf{C}_s$ subgroup of the $\mathbf{I}_h$ is duplicated to afford the value 4 for the $\mathbf{C}'_s$ of the $\mathbf{C}_{2v}$. This vector for the $\mathbf{C}_{2v}$ group is multiplied by the inverse of a mark table for the $\mathbf{C}_{2v}$ group, i. e.,

$$(60\,0\,4\,4\,0)\begin{pmatrix} 1/4 & 0 & 0 & 0 & 0 \\ -1/4 & 1/2 & 0 & 0 & 0 \\ -1/4 & 0 & 1/2 & 0 & 0 \\ -1/4 & 0 & 0 & 1/2 & 0 \\ 1/2 & -1/2 & -1/2 & -1/2 & 1 \end{pmatrix}=(13\,0\,2\,2\,0), \tag{4}$$

Table 3. Subduction of the $\mathbf{I}_h(/\mathbf{C}_s)$ Orbit

$\mathbf{G}_j$	$\mathbf{I}_h(/\mathbf{C}_s)\downarrow\mathbf{G}_j$	USCI-CF	USCI	Sum[a)]
$\mathbf{C}_1$	$60\mathbf{C}_1(/\mathbf{C}_1)$	b_1^{60}	s_1^{60}	1/120
$\mathbf{C}_2$	$30\mathbf{C}_2(/\mathbf{C}_1)$	b_2^{30}	s_2^{30}	1/8
$\mathbf{C}_s$	$28\mathbf{C}_s(/\mathbf{C}_1)+4\mathbf{C}_s(/\mathbf{C}_s)$	$a_1^4c_2^{28}$	$s_1^4s_2^{28}$	1/8
$\mathbf{C}_i$	$30\mathbf{C}_i(/\mathbf{C}_1)$	c_2^{30}	s_2^{30}	1/120
$\mathbf{C}_3$	$20\mathbf{C}_3(/\mathbf{C}_1)$	b_3^{20}	s_3^{20}	1/6
$\mathbf{D}_2$	$15\mathbf{D}_2(/\mathbf{C}_1)$	b_4^{15}	s_4^{15}	0
$\mathbf{C}_{2v}$	$13\mathbf{C}_{2v}(/\mathbf{C}_1)+2\mathbf{C}_{2v}(/\mathbf{C}_s)+2\mathbf{C}_{2v}(/\mathbf{C}_s')$	$a_2^4c_4^{13}$	$s_2^4s_4^{13}$	0
$\mathbf{C}_{2h}$	$14\mathbf{C}_{2h}(/\mathbf{C}_1)+2\mathbf{C}_{2h}(/\mathbf{C}_s)$	$a_2^2c_4^{14}$	$s_2^2s_4^{14}$	0
$\mathbf{C}_5$	$12\mathbf{C}_5(/\mathbf{C}_1)$	b_5^{12}	s_5^{12}	1/5
$\mathbf{D}_3$	$10\mathbf{D}_3(/\mathbf{C}_1)$	b_6^{10}	s_6^{10}	0
$\mathbf{C}_{3v}$	$8\mathbf{C}_{3v}(/\mathbf{C}_1)+4\mathbf{C}_{3v}(/\mathbf{C}_s)$	$a_3^4c_6^8$	$s_3^4s_6^8$	0
$\mathbf{C}_{3i}$	$10\mathbf{C}_{3i}(/\mathbf{C}_1)$	c_6^{10}	s_6^{10}	1/6
$\mathbf{D}_{2h}$	$6\mathbf{D}_{2h}(/\mathbf{C}_1)+\mathbf{D}_{2h}(/\mathbf{C}_s)+\mathbf{D}_{2h}(/\mathbf{C}_s')+\mathbf{D}_{2h}(/\mathbf{C}_s'')$	$a_4^3c_8^6$	$s_4^3s_8^6$	0
$\mathbf{D}_5$	$6\mathbf{D}_5(/\mathbf{C}_1)$	b_{10}^6	s_{10}^6	0
$\mathbf{C}_{5v}$	$4\mathbf{C}_{5v}(/\mathbf{C}_1)+4\mathbf{C}_{5v}(/\mathbf{C}_s)$	$a_5^4c_{10}^4$	$s_5^4s_{10}^4$	0
$\mathbf{C}_{5i}$	$6\mathbf{C}_{5i}(/\mathbf{C}_1)$	c_{10}^6	s_{10}^6	1/5
$\mathbf{T}$	$5\mathbf{T}(/\mathbf{C}_1)$	b_{12}^5	s_{12}^5	0
$\mathbf{D}_{3d}$	$4\mathbf{D}_{3d}(/\mathbf{C}_1)+2\mathbf{D}_{3d}(/\mathbf{C}_s)$	$a_6^2c_{12}^4$	$s_6^2s_{12}^4$	0
$\mathbf{D}_{5d}$	$2\mathbf{D}_{5d}(/\mathbf{C}_1)+2\mathbf{D}_{5d}(/\mathbf{C}_s)$	$a_{10}^2c_{20}^2$	$s_{10}^2s_{20}^2$	0
$\mathbf{T}_h$	$2\mathbf{T}_h(/\mathbf{C}_1)+\mathbf{T}_h(/\mathbf{C}_s)$	$a_{12}c_{24}^2$	$s_{12}s_{24}^2$	0
$\mathbf{I}$	$\mathbf{I}(/\mathbf{C}_1)$	b_{60}	s_{60}	0
$\mathbf{I}_h$	$\mathbf{I}_h(/\mathbf{C}_s)$	a_{60}	s_{60}	0

a) The sum is obtained by summing up each row of the inverse (Table 2).

where the second 5×5 matrix is the inverse. The resulting vector indicates the multiplicity of each CR. Hence, we have

$$\mathbf{I}_h(/\mathbf{C}_s)\downarrow\mathbf{C}_{2v} = 13\mathbf{C}_{2v}(/\mathbf{C}_1)+2\mathbf{C}_{2v}(/\mathbf{C}_s)+2\mathbf{C}_{2v}(/\mathbf{C}_s'). \quad (5)$$

Other subductions are precalculated in a similar way and collected in the second column of Table 3.

According to the subductions, we obtain unit subduced cycle indices (USCIs)[12)] and USCIs with chirality fittingness (USCI-CFs).[20)] In the $\mathbf{C}_{2v}$ group, we assign a variable s_4 (or c_4) to $\mathbf{C}_{2v}(/\mathbf{C}_1)$, s_2 (or a_2) to $\mathbf{C}_{2v}(/\mathbf{C}_s)$, and s_2 (or a_2) to $\mathbf{C}_{2v}(/\mathbf{C}_s')$, where the subscripts come from the equations, $|\mathbf{C}_{2v}|/|\mathbf{C}_1|=4$, $|\mathbf{C}_{2v}|/|\mathbf{C}_s|=2$, and $|\mathbf{C}_{2v}|/|\mathbf{C}_s'|=2$. The variable ($c_4$) is based on the chirality fittingness of the $\mathbf{C}_{2v}(/\mathbf{C}_1)$ (enantiospheric);[18)] the variable (a_2) stems from that of $\mathbf{C}_{2v}(/\mathbf{C}_s)$ or $\mathbf{C}_{2v}(/\mathbf{C}_s')$, which is homospheric. As a result, we have a USCI ($s_2^4s_4^{13}$) and a USCI-CF ($a_2^4c_4^{13}$) in terms of Eq. 5. The other USCIs and USCI-CFs for the $\mathbf{I}_h(/\mathbf{C}_s)$ CR listed in Table 3 are obtained in a similar way.

The above procedure of generating subduced representations is purely algebraic; however, the resulting coset representations of each subgroup have geometrical (or chemical) meaning. In order to convert the skeleton to a $\mathbf{C}_{2v}$-molecule, for example, we start from Eq. 5. This equation indicates that there emerge thirteen 4-membered orbits ($\mathbf{C}_{2v}(/\mathbf{C}_1)$), two 2-membered orbits ($\mathbf{C}_{2v}(/\mathbf{C}_s)$) and two of other 2-membered orbits ($\mathbf{C}_{2v}(/\mathbf{C}_s')$). If these orbits are occupied by different kinds of atoms, we have a $\mathbf{C}_{2v}$ molecule (**7**) with the following packing,

$$\underbrace{\mathrm{X_2Y_2}}_{\text{2 kinds}} \quad \underbrace{\mathrm{Z_2W_2}}_{\text{2 kinds}} \quad \underbrace{\mathrm{H_4\cdots B_4}}_{\text{13 kinds}} \qquad (6)$$

The first block of this equation corresponds to the 2-membered orbits of $\mathbf{C}_{2v}(/\mathbf{C}_s)$, where ●=X and ○=Y. These vertices are fixed during a reflection concerning the mirror plane that contains ●'s and ○'s. The second block of Eq. 6 is concerned with the 2-membered orbits of $\mathbf{C}_{2v}(/\mathbf{C}_s')$, where △=Z and ▲=W. These vertices are contained in the mirror plane associated with the $\mathbf{C}_s'$ group. The third block of Eq. 6 indicates a mode of packing in the remaining 13 orbits, some of which are, for example, differentiated by distinct marks. Although there exist $\mathbf{C}_{2v}$ molecules (**8**—**10**) having the formula ($\mathrm{C_{60}H_{56}X_2Y_2}$), their orbits are also controlled by Eq. 5. In other words, the 56 hydrogen atoms are classified into 15 equivalence classes (orbits).

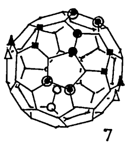
7

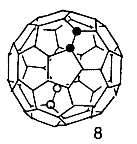
8

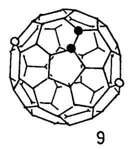
9

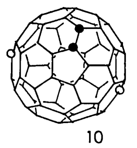
10

Figure 2 depicts a representative molecule for every subgroup of $\mathbf{I}_h$, where ● and ○ denote X and Y; and

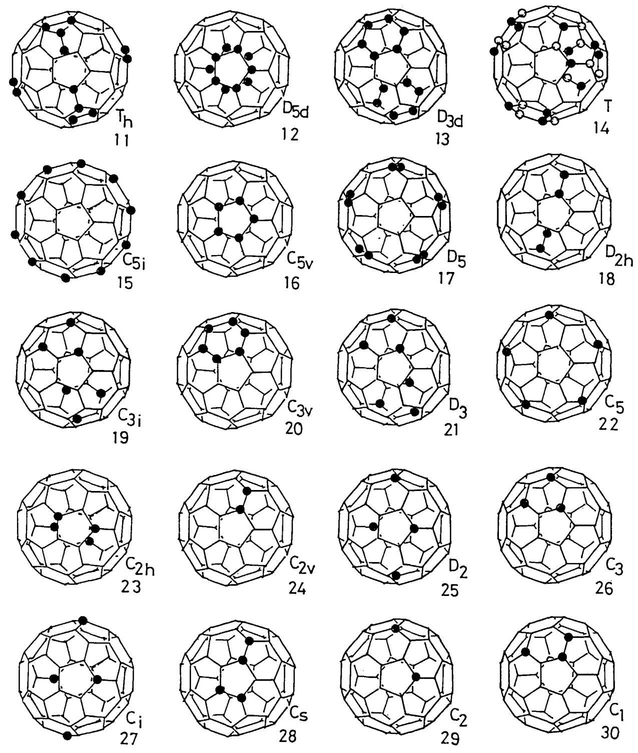

Fig. 2. Molecules derived from the soccerane skeleton (**1**).

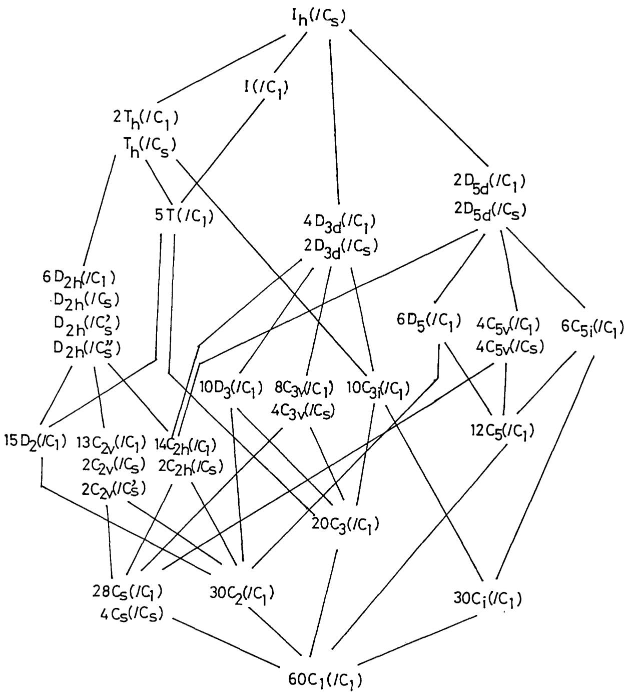

Fig. 3. Desymmetrization lattice for $I_h(/C_s)$.

unmarked vertices take hydrogen atoms. The orbits of each of the molecules are subject to the subduction listed in Table 1.

Since any derivation based on the soccerane skeleton (**1**) is regarded as a desymmetrization of the skeleton, the derivation can be determined systematically in terms of a desymmetrization lattice[18] for the $I_h(/C_s)$ (Fig. 3). This figure depicts a group-subgroup lattice for the I_h group which accompanies the results of subduction listed in Table 3.

The absence of a molecule of a subgroup is determined by examining its supergroups: if one of the supergroups has the same USCI as that of the subgroup at issue, the molecule does not exist. This determination can also be accomplished by using the subduction data in Fig. 3. In the present case, the CR $I(/C_1)$ corresponds to a 60-membered orbit, whose size is equal to that of an $I_h(/C_s)$ orbit. Hence, **I**-molecules are absent; all of the remaining subgroups are possible to exist for the soccerane series. This conclusion can be obtained more conveniently by comparing the corresponding USCIs; the USCI of the $I(/C_1)$ orbit is s_{60}, which is equl to that of the $I_h(/C_s)$ orbit. On the other hand, the absence of C_5-, D_5-, C_{5i}-, and **I**-molecules has been reported for dodecahedrane derivatives having an $I_h(/C_{3v})$ orbit.[16]

3. Soccerane Derivatives with Achiral Substituents. In the preceding section, we have qualitatively examined the desymmetrizations of the soccerane skeleton (**1**) that create derivatives of various subsymmetries. The next issue is to calculate the number of such derivatives. Since the 60 vertices of saccerane (**3**) construct an orbit that is subject to $I_h(/C_s)$, we use the USCIs listed in Table 3 as the corresponding subduced cycle indices (SCIs).[12] We consider H and X as substituents. This corresponds to a figure inventory expressed by

$$s_d = 1 + x^d. \tag{7}$$

This was introduced into the SCIs to provide the following generating functions,

$$s_1^{60} = (1 + x)^{60} \text{ for } C_1, \tag{8}$$

$$s_2^{30} = (1 + x^2)^{30} \text{ for } C_2, \tag{9}$$

$$s_1^4 s_2^{28} = (1 + x)^4 (1 + x^2)^{28} \text{ for } C_s, \tag{10}$$

$$s_2^{30} = (1 + x^2)^{30} \text{ for } C_i, \tag{11}$$

$$s_3^{20} = (1 + x^3)^{20} \text{ for } C_3, \tag{12}$$

$$s_4^{15} = (1 + x^4)^{15} \text{ for } D_2, \tag{13}$$

$$s_2^4 s_4^{13} = (1 + x^2)^4 (1 + x^4)^{13} \text{ for } C_{2v}, \tag{14}$$

$$s_2^2 s_4^{14} = (1 + x^2)^2 (1 + x^4)^{14} \text{ for } C_{2h}, \tag{15}$$

$$s_5^{12} = (1 + x^5)^{12} \text{ for } C_5, \tag{16}$$

$$s_6^{10} = (1 + x^6)^{10} \text{ for } D_3, \tag{17}$$

$$s_3^4 s_6^8 = (1 + x^3)^4 (1 + x^6)^8 \text{ for } C_{3v}, \tag{18}$$

$$s_6^{10} = (1 + x^6)^{10} \text{ for } \mathbf{C}_{3i}, \tag{19}$$

$$s_4^3 s_8^6 = (1 + x^4)^3 (1 + x^8)^6 \text{ for } \mathbf{D}_{2h}, \tag{20}$$

$$s_{10}^6 = (1 + x^{10})^6 \text{ for } \mathbf{D}_5, \tag{21}$$

$$s_5^4 s_{10}^4 = (1 + x^5)^4 (1 + x^{10})^4 \text{ for } \mathbf{C}_{5v}, \tag{22}$$

$$s_{10}^6 = (1 + x^{10})^6 \text{ for } \mathbf{C}_{5i}, \tag{23}$$

$$s_{12}^5 = (1 + x^{12})^5 \text{ for } \mathbf{T}, \tag{24}$$

$$s_6^2 s_{12}^4 = (1 + x^6)^2 (1 + x^{12})^4 \text{ for } \mathbf{D}_{3d}, \tag{25}$$

$$s_{10}^2 s_{20}^2 = (1 + x^{10})^2 (1 + x^{20})^2 \text{ for } \mathbf{D}_{5d}, \tag{26}$$

$$s_{12} s_{24}^2 = (1 + x^{12})(1 + x^{24})^2 \text{ for } \mathbf{T}_h, \tag{27}$$

$$s_{60} = 1 + x^{60} \text{ for } \mathbf{I}, \tag{28}$$

and

$$s_{60} = 1 + x^{60} \text{ for } \mathbf{I}_h. \tag{29}$$

After expanding these generating functions, the resulting coefficients are collected to give a matrix, each row of which consists of the coefficients of the term x^m (m=0 to 60). Since the coefficient of the term x^m is equal to that of x^{60-m}, we refer to them as being complementary. In the following discussions, therefore, we take account of the term x^m ($m \leqslant 30$) mainly. The next step is the multiplication of matrix by the inverse of the mark table.[16] For explaining this step, let us examine the term x^{12} only. The corresponding row of the matrix is equal to (1399358844975, 593775, 986895, 593775, 4845, 455, 767, 455, 0, 45, 77, 45, 19, 0, 0, 0, 5, 5, 0, 1, 0, 0). When we multiply this row vector by the inverse (Table 2), we have a row vector (11661121142, 148014, 246200, 9781, 1170, 72, 374, 213, 0, 20, 36, 19, 6, 0, 0, 0, 2, 5, 0, 1, 0, 0), which is listed in the x^{12} (or x^{48}) row of Table 4. These values are aligned in the order of the SSG of the $\mathbf{I}_h$ group. Thus, there emerge 11661121142 $\mathbf{C}_1$-, 148014 $\mathbf{C}_2$-, 246200 $\mathbf{C}_s$-, 9781 $\mathbf{C}_i$-, 1170 $\mathbf{C}_3$-, 72 $\mathbf{D}_2$-, 374 $\mathbf{C}_{2v}$-, 213 $\mathbf{C}_{2h}$-, 20 $\mathbf{D}_3$-, 36 $\mathbf{C}_{3v}$-, 19 $\mathbf{C}_{3i}$-, 6 $\mathbf{D}_{2h}$-, 2 $\mathbf{T}$-, 5 $\mathbf{D}_{3d}$-, and one $\mathbf{T}_h$-isomers, all of which have the molecular formula $C_{60}H_{48}X_{12}$. The other rows of Table 4 are calculated in a similar way. It should be emphasized that these enumerations (Table 4) produce molecules having $\mathbf{C}_5$, $\mathbf{D}_5$, and $\mathbf{C}_{5i}$ symmetries, whereas the dodecahedrane skeleton cannot produce these symmetries.[16] The absence of $\mathbf{I}$-derivatives is verified by these enumerations.

Figure 4 depicts $\mathbf{T}$ molecules, the numbers of which are calculated to be equal to 2 for the term x^{12} and 4 for the term x^{24}. The first two molecules (**31** and **32**) correspond to x^{12}. Note that we depict an arbitrary representative selected from each pair of enantiomers. The alternate labeling in each of the four 6-membered

Table 4. The Numbers of Derivatives from **1** with H and X

Term	Numbers of derivatives in the order of SSG
$1, x^{60}$	0, 0, 0, 0, 0, 0, 0, 0, 0, 0, 0, 0, 0, 0, 0, 0, 0, 0, 0, 0, 1
x, x^{59}	0, 0, 1, 0, 0, 0, 0, 0, 0, 0, 0, 0, 0, 0, 0, 0, 0, 0, 0, 0, 0
x^2, x^{58}	8, 6, 6, 0, 0, 0, 2, 1, 0, 0, 0, 0, 0, 0, 0, 0, 0, 0, 0, 0, 0,
x^3, x^{57}	270, 0, 27, 0, 4, 0, 0, 0, 0, 0, 2, 0, 0, 0, 0, 0, 0, 0, 0, 0, 0
x^4, x^{56}	3946, 98, 125, 4, 0, 2, 8, 6, 0, 0, 0, 0, 1, 0, 0, 0, 0, 0, 0, 0, 0
x^5, x^{55}	45310, 0, 404, 0, 0, 0, 0, 0, 2, 0, 0, 0, 0, 0, 2, 0, 0, 0, 0, 0, 0, 0
x^6, x^{54}	415972, 990, 1352, 60, 40, 0, 28, 12, 0, 4, 6, 4, 0, 0, 0, 0, 0, 2, 0, 0, 0, 0
x^7, x^{53}	3216564, 0, 3654, 0, 0, 0, 0, 0, 0, 0, 0, 0, 0, 0, 0, 0, 0, 0, 0, 0, 0
x^8, x^{52}	21313194, 6764, 10027, 432, 0, 16, 74, 48, 0, 0, 0, 0, 3, 0, 0, 0, 0, 0, 0, 0, 0
x^9, x^{51}	123180894, 0, 23733, 0, 276, 0, 0, 0, 0, 0, 18, 0, 0, 0, 0, 0, 0, 0, 0, 0, 0
x^{10}, x^{50}	628236648, 35488, 55870, 2330, 0, 0, 182, 89, 12, 0, 0, 0, 0, 2, 4, 2, 0, 0, 2, 0, 0, 0
x^{11}, x^{49}	2855775000, 0, 118755, 0, 0, 0, 0, 0, 0, 0, 0, 0, 0, 0, 0, 0, 0, 0, 0, 0, 0
x^{12}, x^{48}	11661121142, 148014, 246200, 9781, 1170, 72, 374, 213, 0, 20, 36, 19, 6, 0, 0, 0, 2, 5, 0, 1, 0, 0
x^{13}, x^{47}	43056957720, 0, 475020, 0, 0, 0, 0, 0, 0, 0, 0, 0, 0, 0, 0, 0, 0, 0, 0, 0, 0
x^{14}, x^{46}	144548441676, 508404, 884780, 33748, 0, 0, 728, 364, 0, 0, 0, 0, 0, 0, 0, 0, 0, 0, 0, 0, 0, 0
x^{15}, x^{45}	443283294954, 0, 1560698, 0, 3840, 0, 0, 0, 50, 0, 72, 0, 0, 0, 10, 0, 0, 0, 0, 0, 0
x^{16}, x^{44}	1246734362500, 1461938, 2645692, 97213, 0, 222, 1238, 666, 0, 0, 0, 0, 11, 0, 0, 0, 0, 0, 0, 0, 0
x^{17}, x^{43}	3226845176280, 0, 4292145, 0, 0, 0, 0, 0, 0, 0, 0, 0, 0, 0, 0, 0, 0, 0, 0, 0, 0
x^{18}, x^{42}	7708574462808, 3575230, 6682278, 237936, 9576, 0, 2002, 993, 0, 56, 112, 56, 0, 0, 0, 0, 0, 8, 0, 0, 0, 0
x^{19}, x^{41}	17040013308780, 0, 10015005, 0, 0, 0, 0, 0, 0, 0, 0, 0, 0, 0, 0, 0, 0, 0, 0, 0, 0
x^{20}, x^{40}	34932026335736, 7508306, 14414483, 500008, 0, 492, 2906, 1473, 110, 0, 0, 0, 17, 6, 14, 6, 0, 0, 3, 0, 0, 0
x^{21}, x^{39}	66537204356484, 0, 20029842, 0, 19296, 0, 0, 0, 0, 0, 168, 0, 0, 0, 0, 0, 0, 0, 0, 0, 0
x^{22}, x^{38}	117952313908338, 13653822, 26774930, 909454, 0, 0, 4004, 2002, 0, 0, 0, 0, 0, 0, 0, 0, 0, 0, 0, 0, 0, 0
x^{23}, x^{37}	194877752875260, 0, 34597290, 0, 0, 0, 0, 0, 0, 0, 0, 0, 0, 0, 0, 0, 0, 0, 0, 0, 0
x^{24}, x^{36}	300436529264126, 21618198, 43090979, 1440284, 31280, 822, 5044, 2460, 0, 100, 212, 98, 21, 0, 0, 0, 4, 10, 0, 2, 0, 0
x^{25}, x^{35}	432628623838072, 0, 51895915, 0, 0, 0, 0, 0, 188, 0, 0, 0, 0, 0, 20, 0, 0, 0, 0, 0, 0, 0
x^{26}, x^{34}	582384674721528, 29935458, 60354210, 1994496, 0, 0, 6006, 3003, 0, 0, 0, 0, 0, 0, 0, 0, 0, 0, 0, 0, 0, 0
x^{27}, x^{33}	733373318255628, 0, 67863663, 0, 41864, 0, 0, 0, 0, 0, 252, 0, 0, 0, 0, 0, 0, 0, 0, 0, 0
x^{28}, x^{32}	864332823097128, 36349164, 73789608, 2422115, 0, 1060, 6612, 3180, 0, 0, 0, 0, 25, 0, 0, 0, 0, 0, 0, 0, 0
x^{29}, x^{31}	953746586743696, 0, 77558760, 0, 0, 0, 0, 0, 0, 0, 0, 0, 0, 0, 0, 0, 0, 0, 0, 0, 0
x^{30}	985538119566784, 38774104, 78887120, 2583540, 45936, 0, 6864, 3416, 212, 120, 260, 120, 0, 8, 20, 8, 0, 12, 4, 0, 0, 0

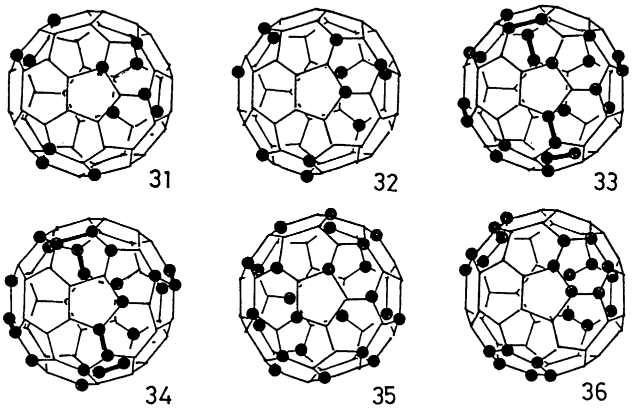

Fig. 4. **T**-Molecules derived from **1** with H and X.

rings of **31** is given just in an inverse fashion as compared with that in the counterpart of **32**. The remaining four (**33**—**36**) have the common molecular formula ($C_{60}H_{36}X_{24}$). The molecule (**33**) can be considered to come from a superposition of **11** and **31**, where heavy lines are tentatively given to show the contribution of **11**. In a similar way, the molecule (**34**) stems from a superposition of **11** and **32**. The molecule (**35**) is created by superposing **31** onto **32** so as to retain the **T**-symmetry. This superposition can be understood by focusing our attention on the eight hexagonal faces. The molecule (**36**) is generated by another mode of superposition of **31** and **32**. In accord with the qualitative discussion in the preceding section, each of these molecules has orbits that are controlled by the subduction listed in Table 3.

Molecules of $\mathbf{T}_h$ symmetry have been scarcely demonstrated by most textbooks of stereochemistry or of chemical group theory. The present enumeration provides us with suitable examples of such $\mathbf{T}_h$ molecules. Thus, there emerge three $\mathbf{T}_h$ molecules (one molecule (**11**) for x^{12} and two for x^{24}). The remaining two are depicted in Fig. 5. Comparisons of **35** (**T**) with **37** ($\mathbf{T}_h$) and with **38** ($\mathbf{T}_h$) afford their interrelation, if we pay attention to the respective eight hexagonal faces.

Figure 6 collects $\mathbf{D}_5$ molecules appearing in this enumeration. Among them, the two molecules (**17** and **39**) correspond to the term x^{10} ($C_{60}H_{50}X_{10}$) or the complementary x^{50} ($C_{60}H_{10}X_{50}$); the six isomers (**40**—**45**) are concerned with the term x^{20} ($C_{60}H_{40}X_{20}$) or the complementary x^{40} ($C_{60}H_{20}X_{40}$); and the 8 isomers (**46**—**53**) agree with the term x^{30} ($C_{60}H_{30}X_{30}$). All these molecules have a five-fold axis perpendicular to the page as well as five two-fold axes all perpendicular to the five-fold axis.

The total number of derivatives with each molecular formula is calculated in the form of a generating function.[21] Here, we give some comments to the previous results. According to Theorem 4 and Lemma 1 in our paper,[12] the number of isomers with W_θ-weight and $\mathbf{G}_i$-symmetry is represented by

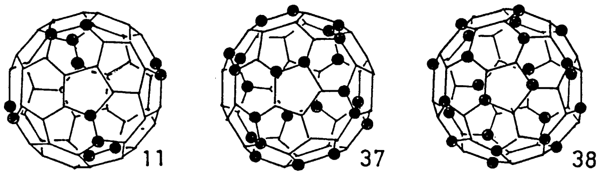

Fig. 5. $\mathbf{T}_h$-Molecules derived from **1** with H and X.

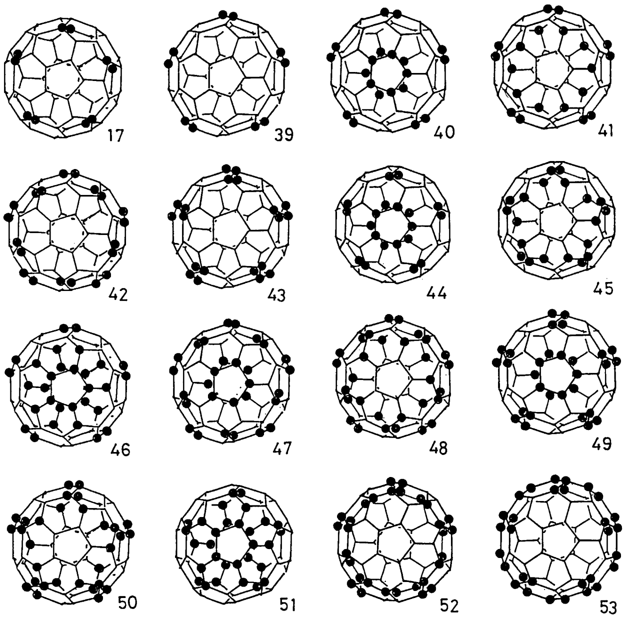

Fig. 6. $\mathbf{D}_5$-Molecules derived from **1** with H and X.

$$A_{\theta i} = \sum_{j=1}^{s} \rho_{\theta j}\overline{m}_{ji} \text{ (for } i=1,2,\cdots, s, j=1,2,\cdots,s) \tag{30}$$

where the symbol $\rho_{\theta j}$ denotes the number of fixed configurations and $\overline{m}_{ji}$ is the jith element of the inverse of the mark table for **G** group. If we tantatively fix $\mathbf{G}_i$-symmetry, then we have

$$\begin{aligned}\sum_{[\theta]} A_{\theta i} W_\theta &= \sum_{[\theta]} \sum_{j=1}^{s} \rho_{\theta j}\overline{m}_{ji} W_\theta \\ &= \sum_{j=1}^{s} \overline{m}_{ji} \sum_{[\theta]} \rho_{\theta j} W_\theta \\ &= \sum_{j=1}^{s} \overline{m}_{ji}\, ZI(\mathbf{G}_j; s_{d_{jk}}^{i\alpha}).\end{aligned} \tag{31}$$

The last equation is derived from the fact that the summation ($\sum_{[\theta]}\rho_{\theta j} W_\theta$) is a generating function of $\rho_{\theta i}$. This is in turn given by Lemma 1 of the paper[12] to be

$$\sum_{[\theta]} \rho_{\theta j} W_\theta = ZI(\mathbf{G}_j; s_{d_{jk}}^{i\alpha}), \tag{32}$$

where the right-hand side is a subduced cycle index (SCI) and $s_{d_{jk}}^{i\alpha}$ is replaced by

$$s_{d_{jk}}^{i\alpha} = \sum_{r=1}^{|X|} w_{i\alpha}(X_r)^{d_{jk}}. \tag{33}$$

We here introduce a *partial cycle index* by means of the following definition.

Definition 1. A *partial cycle index for* $\mathbf{G}_i$ *group* is defined as

$$\mathrm{PCI}(\mathbf{G}_i;\, s_{d_{jk}}^{i\alpha}) = \sum_{j=1}^{s} \overline{m}_{ji}\, ZI(\mathbf{G}_j;\, s_{d_{jk}}^{i\alpha})(\text{for } i=1,2,\cdots, s). \tag{34}$$

When we introducte the PCI into Eq. 31, we have the following theorem.

Theorem 1. The number of isomers with W_θ-weight and $\mathbf{G}_i$-symmetry is obtained as a coefficient of the equation,

$$\sum_{[\theta]} A_{\theta i} W_\theta = \mathrm{PCI}(\mathbf{G}_j;\, s_{d_{jk}}^{i\alpha})(\text{for } i=1,2,\cdots, s), \tag{35}$$

where the right-hand side a partial cycle index (PCI) and $s_{d_{jk}}^{i\alpha}$ is replaced by

$$s_{d_{jk}}^{i\alpha} = \sum_{r=1}^{|\mathrm{X}|} w_{i\alpha}(X_r)^{d_{jk}}. \tag{36}$$

In order to count $\mathbf{C}_{2\mathrm{v}}$-derivatives of soccerane, we have the following PCI from the data of Tables 2 and 3 by means of Eq. 34.

$$\mathrm{PCI}(\mathbf{C}_{2\mathrm{v}},\, s_d) = (1/2)s_2^4 s_4^{13} - (1/2)s_4^3 s_8^6. \tag{37}$$

In this equation, we find that the terms corresponding to the $\mathbf{C}_{2\mathrm{v}}$- and $\mathbf{D}_{2\mathrm{h}}$-rows are effective in the light of the $\mathbf{I}_\mathrm{h}(/\mathbf{C}_{2\mathrm{v}})$-column of Table 2. Introducing the figure inventory (Eq. 7) in Eq. 37, we obtain the numbers of $\mathbf{C}_{2\mathrm{v}}$-derivatives itemized with respect to molecular formulas. They are identical to the values of the $\mathbf{C}_{2\mathrm{v}}$ subgroup listed in Table 4. In a similar way, we can obtain a PCI and a generating function of calculating numbers of isomers for every subgroups. Since Theorem 1 is a generating-function version of Theorem 4 of the previous paper,[12] there appear no new matters beyond the previous theorem. A similar generating function has been obtained alternatively by Kerber and Thürlings,[22] though their formulation does not contain the concepts of USCIs, SCI and PCI and take no account of obligatory minimum valency.

By using the PCI, we introduce an alternative definition of a cycle index (CI):

$$\mathrm{CI} = \sum_{j=1}^{s} \mathrm{PCI}(\mathbf{G}_j;\, s_{d_{jk}}^{i\alpha}). \tag{38}$$

This is equivalent to our previous result,[21] i. e.,

$$\mathrm{CI} = \sum_{j=1}^{s} (\sum_{i=1}^{s} \overline{m}_{ji}) ZI(\mathbf{G}_j;\, s_{d_{jk}}^{i\alpha}). \tag{39}$$

The cycle index (CI) corresponding to the present case is obtained by using the data of Table 3, i. e.,

$$\begin{aligned}\mathrm{CI}(\mathbf{I}_\mathrm{h};\, s_d) = {} & (1/120)s_1^{60} + (1/8)s_2^{30} + (1/8)s_1^4 s_2^{28} + (1/120)s_2^{30} \\ & + (1/6)s_3^{20} + (1/5)s_5^{12} + (1/6)s_6^{10} + (1/5)s_{10}^6,\end{aligned} \tag{40}$$

where the coefficients of the term in the right-hand side are adopted from the rightmost column of Table 2 or 3. This derivation of the CI is based on such a theorem that is different from Pólya's one. However, these two theorems have been proven to afford the same CI in general.[21] If we introduce the figure inventory (Eq. 7) into the cycle index (Eq. 40), we have the generating function,

$$\begin{aligned} Z(x) = {} & \mathrm{CI}(\mathbf{I}_\mathrm{h};\, 1 + x^d) \\ = {} & (x^0 + x^{60}) + (x^1 + x^{59}) + 23(x^2 + x^{58}) \\ & + 303(x^3 + x^{57}) + 4190(x^4 + x^{56}) \\ & + 45718(x^5 + x^{55}) + 418470(x^6 + x^{54}) \\ & + 3220218(x^7 + x^{53}) + 21330558(x^8 + x^{52}) \\ & + 123204921(x^9 + x^{51}) + 628330629(x^{10} + x^{50}) \\ & + 2855893755(x^{11} + x^{49}) + 11661527055(x^{12} + x^{48}) \\ & + 43057432740(x^{13} + x^{47}) + 144549869700(x^{14} + x^{46}) \\ & + 443284859624(x^{15} + x^{45}) + 1246738569480(x^{16} + x^{44}) \\ & + 3226849468425(x^{17} + x^{43}) + 7708584971055(x^{18} + x^{42}) \\ & + 17040023323785(x^{19} + x^{41}) + 34932048763560(x^{20} + x^{40}) \\ & + 66537224405790(x^{21} + x^{39}) \\ & + 117952355252550(x^{22} + x^{38}) \\ & + 194877787472550(x^{23} + x^{37}) \\ & + 300436595453640(x^{24} + x^{36}) \\ & + 432628675734195(x^{25} + x^{35}) \\ & + 582384767014701(x^{26} + x^{34}) \\ & + 733373386161407(x^{27} + x^{33}) \\ & + 864332935668892(x^{28} + x^{32}) \\ & + 953746664302456(x^{29} + x^{31}) + 985538239868528x^{30}. \end{aligned} \tag{41}$$

The coefficient of each term is identical with the value that is calculated by the direct summation of the corresponding row of Table 4.

It is worthwhile mentioning the difference between Hosoya's enumeration[10] and the present one (Eq. 41). Since Hosoya has used **I** group for obtaining a CI, both enantiomers of a racemic pair are counted in as two isomers. For example, he has reported that the coefficient of the term x^2 is equal to 37, while our result (Eq. 41) contains $23x^2$. Note that our enumeration uses $\mathbf{I}_\mathrm{h}$ group and counts each pair of enantiomers once. Since our enumeration affords such values that are itemized with respect to the terms as well as to the subsymmetries, the Hosoya's value can be calculated in terms of the data listed in Table 4. Thus, the x^2 row of Table 4 affords the expression, $8\times2+6\times2+6+2+1=37$, where the values in the left-hand side are duplicated if they are concerned with chiral subgroups. The value in the right-hand side is equal to the Hosoya's one. Compare this with $8+6+6+2+1=23$ for our result, which no such duplication is taken into account.

4. Conclusion. The 60 vertices of soccerane belong to an $\mathbf{I}_\mathrm{h}(/\mathbf{C}_\mathrm{s})$ orbit. Desymmetrization of this orbit by every subgroup ($\mathbf{G}_j$) of $\mathbf{I}_\mathrm{h}$ is characterized by the subduced representation ($\mathbf{I}_\mathrm{h}(/\mathbf{C}_\mathrm{s})\downarrow\mathbf{G}_j$). This representation is reduced to the sum of the coset representations of the $\mathbf{G}_j$ group. This subduction affords a unit subduced cycle index (USCI), which is useful for enumeration of derivatives starting from the soccerane skeleton. The enumeration indicates the versatility of the USCI approach. Although the enumeration is restricted to the soccerane skeleton (the $\mathbf{I}_h(/\mathbf{C}_s)$ orbit), the USCI method can be applied to any other skeletons of the $\mathbf{I}_h$ symmetry (Table 1).

References

1) a) P. E. Eaton, *Tetrahedron,* **35**, 2189 (1979). b) K. Naemura, *Yuki Gosei Kagaku Kyokai Shi,* **45**, 48 (1987). c) L. A. Paquette, *Chem. Rev.,* **89**, 1051 (1989).

2) E. Osawa, *Kagaku (Kyoto),* **25**, 854 (1970).

3) J. Castells and F. Serratosa, *J. Chem. Educ.,* **60**, 941 (1983).

4) J. Castells and F. Serratosa, *J. Chem. Educ.,* **63**, 630 (1986).

5) a) H. W. Kroto, J. R. Heath, S. C. O'Brien, and R. E. Smalley, *Nature,* **318**, 162 (1985). b) Y. Liu, S. C. O'Brien, Q. L. Zhang, J. R. Heath, F. K. Tittle, R. F. Curl, H. W. Kroto, and R. E. Smalley, *Chem. Phys. Lett.,* **126**, 215 (1986). c) Q. L. Zhang, S. C. O'Brien, J. R. Heath, Y. Liu, R. F. Curl, H. W. Kroto, and R. E. Smalley, *J. Phys. Chem.,* **90**, 525 (1986).

6) We adopt the name *soccerane* for referring to this compound (or cluster) after Castells' proposal.[3] Kroto et al.[5a] have once referred to this cluster as "buckminsterfullerene"; however, Buckminster Fuller's architecture has been pointed out to be based on organized triangles, not on such a truncated icosahedron.[10]

7) a) D. J. Klein, T. G. Schmalz, G. E. Hite, and W. A. Seitz, *J. Am. Chem. Soc.,* **108**, 1301 (1986). b) Z. Slanina, J. M. Rudzinski, and E. Osawa, *Coll. Czech. Chem. Commun.,* **52**, 2831 (1987). c) R. C. Haddon, L. E. Brus, and K. Raghavachari, *Chem. Phys. Lett.,* **125**, 459 (1986). d) R. L. Disch and J. M. Schulman, *Chem. Phys. Lett.,* **125**, 465 (1986). e) P. W. Fowler, *Chem. Phys. Lett.,* **131**, 444 (1986). f) H. P. Lüthi and J. Almlöf, *Chem. Phys. Lett.,* **135**, 357 (1987). g) G. W. Hayden and E. J. Mele, *Phys. Rev. B,* **36**, 5010 (1987). h) A. J. Stone and D. J. Wales, *Chem. Phys. Lett.,* **128**, 501 (1986). i) A. D. J. Haymet, *J. Am. Chem. Soc.,* **108**, 319 (1986).

8) a) A. D. J. Haymet, *Chem. Phys. Lett.,* **122**, 421 (1985). b) P. W. Fowler and J. Woolrich, *J. Chem. Phys. Lett.,* **127**, 78 (1986). c) J. M. Schulman, R. L. Disch, M. A. Miller, and R. C. Peck, *Chem. Phys. Lett.,* **141**, 45 (1987). d) T. Shibuya and M. Yoshitani, *Chem. Phys. Lett.,* **137**, 13 (1987).

9) E. Osawa, *Kagaku (Kyoto),* **42**, 62 (1987).

10) H. Hosoya, *Gendai-Kagaku,* **201**, 38 (1987). See also O. Knop, W. W. Barker, and P. S. White, *Acta Crystallogr., Sect. A,* **31**, 461 (1975).

11) a) G. Pólya, *Acta Math.,* **68**, 145 (1937). b) G. Pólya, "Combinatorial Enumeration of Groups, Graphs, and Chemical Compounds," Springer-Verlag, New York-Berlin-Heidelberg (1987).

12) S. Fujita, *Theor. Chim. Acta,* **76**, 247 (1989).

13) For other enumeration methods, see a) J. Sheehan, *Can. J. Math.,* **20**, 1068 (1968). b) W. Hässelbarth, *Theor. Chim. Acta,* **67**, 339 (1985). c) J. Brocas, *J. Am. Chem. Soc.,* **108**, 1135 (1986). d) C. A. Mead, *J. Am. Chem. Soc.,* **109**, 2130 (1987).

14) W. Burnside, "Theory of Groups of Finite Order," 2nd ed, Cambridge Univ. Press, Cambridge (1911).

15) a) S. Fujita, *Bull. Chem. Soc. Jpn.,* **62**, 3771 (1989). b) S. Fujita, *Bull. Chem. Soc. Jpn.,* **63**, 203 (1989). c) S. Fujita, *Tetrahedron,* **46**, 365 (1989). d) S. Fujita, *Bull. Chem. Soc. Jpn.,* **63**, 1876 (1989), e) *ibid.,* **63**, 2033 (1989).

16) S. Fujita, *Bull. Chem. Soc. Jpn.,* **63**, 2759 (1990).

17) S. Fujita, *Bull. Chem. Soc. Jpn.,* **63**, 315 (1990).

18) S. Fujita, *J. Am. Chem. Soc.,* **112**, 3390 (1990).

19) A. full mark table for $\mathbf{I}_h$ group has been reported elsewhere.[16]

20) S. Fujita, *J. Math. Chem.,* **5**, 121 (1990).

21) S. Fujita, *J. Math. Chem.,* **5**, 99 (1990).

22) A. Kerber and K. -J. Thürlings, in "Lecture Notes in Mathematics," Springer, New York (1982), Vol. 969, p. 191.